the line shape, we must now treat Eq. (88) in the same way we treated (62). But (88) represents an enormous simplification over (62) since we now have only one state where we used to have $(2j+1)$, and the order of all matrices that enter into the calculation is correspondingly reduced.

The matrix h defined by (84) vanishes whenever the angular momenta j_a and j_α differ by more than one unit, whenever j_b and j_β differ by more than one unit, and whenever the product of the parities of a and α differs from that of b and β. The matrix δ defined by (87) may be taken to vanish under exactly the same circumstances and, in addition, it vanishes unless the parities of a and α differ and those of b and β differ too. As a consequence, the only doubled reduced states that need to be considered in the calculation of (88) are those for which the angular momentum of the final state does not differ by more than one unit from the angular momentum of the initial state, and for which the two parities are different. In other words, we only need to consider doubled states that correspond to actually observed lines in the spectrum of the atom. Thus, the work of Sec. 6 is further simplified.

The "reduction to collision axes" is possible also here, as in the one-state case. When we calculate $\mathfrak{K}$ by (61), it is not necessary to average over all possible orientations of the collision. It is sufficient to compute $\mathfrak{K}$ with a convenient set of "collision axes." The summation in (84) does the averaging over all directions for us. This is because $((a\alpha^+|h|b\beta^+))$ is independent of any magnetic quantum number, and hence it will be the same for any orientation of the collision. It is easy to see, with the help of (80) and (81), that the two-state case of (61) and (84) reduces to the one-state case of (28) and (73) whenever one of the two components of a line is unaffected by the collisions.

PHYSICAL REVIEW VOLUME 111, NUMBER 2 JULY 15, 1958

Photodetachment Cross Section and the Electron Affinity of Atomic Oxygen*

LEWIS M. BRANSCOMB, DAVID S. BURCH, STEPHEN J. SMITH, AND SYDNEY GELTMAN
National Bureau of Standards, Washington, D. C.

(Received February 14, 1958)

Experiments and theory on the continuous absorption of radiation by atomic-oxygen negative ions are described and discussed. The absorption cross section for photon energies not too near threshold is obtained directly from one of the experiments. Theory and experiment are combined to give the cross section in the vicinity of threshold and a precise value of the electron affinity of atomic oxygen. The latter result is EA(O) $=1.465\pm0.005$ ev. The data are used for computation of the radiative attachment coefficient, and other applications of the experimental results are discussed.

INTRODUCTION

THE absorption of continuous radiation by the O^- ion leads to the photodetachment of the extra electron.[1,2] This process is partially responsible for the release of electrons and the destruction of negative ions in the sunlit ionosphere,[3] and provides a source of opacity in certain spectral ranges for high-temperature plasmas containing oxygen.[4] The potential astrophysical importance of O^- absorption is suggested by the influence of H^- photodetachment on the solar continuous spectrum.[5] Comparison of the experimental photodetachment cross section with values calculated using approximate atomic wave functions and potentials may be helpful in the theoretical study of related processes less susceptible to experiment, for example, elastic scattering of electrons by atomic oxygen.[6] From the photodetachment cross section one can compute the radiative attachment cross section by the principle of detailed balancing. Radiative attachment provides the limiting rate for ion formation at low pressures.

The photon energy E_0 at the threshold for continuous absorption from the lowest state of O^- to the lowest state of O is equal to the binding energy of the ion and hence to the physical electron affinity of the oxygen atom. Observation of this threshold then provides a direct method for determining the oxygen affinity, EA(O). An accurate value for this affinity is needed both for the interpretation of physical processes involving O^- and for determination of other thermochemical constants numerically related to the oxygen electron affinity.

Previous determinations of EA(O) from the photo-

* This work was supported in part by the Office of Naval Research.

[1] H. S. W. Massey, *Negative Ions* (Cambridge University Press, New York, 1950), second edition, p. 84 ff.

[2] Lewis M. Branscomb, *Advances in Electronics and Electron Physics* (Academic Press, Inc., New York, 1957), first edition, Vol. 9, p. 43.

[3] D. R. Bates and H. S. W. Massey, J. Atmospheric and Terrest. Phys. 2, 1 (1951).

[4] R. E. Meyerott, *The Threshold of Space* (Pergamon Press, London, 1957), first edition, p. 259.

[5] R. Wildt and S. Chandrasekhar, Astrophys. J. **100**, 87 (1944).

[6] L. B. Robinson, Phys. Rev. **105**, 922 (1957); Hammerling, Shine, and Kivel, J. Appl. Phys. **28**, 760 (1957); A. Temkin, Phys. Rev. **107**, 1004 (1957); T. Yamanouchi, Progr. Theoret. Phys. (Japan) **2**, 33 (1947).

detachment threshold gave the values[7,8] 1.45±0.15 ev and 1.48±0.10 ev. These results are in good agreement with determinations based on thresholds for O^- production by electron impact, providing the latter are interpreted using the correct molecular dissociation energies,[9] but disagree with the studies of electron attachment at a hot filament.[10,11] From NO, Clarke[12] found EA(O)=1.50±0.2 ev, and Kerwin[13] points out that an even more precise value can be calculated from the appearance potential for N^+ and O^- ions in Clarke's data by using $I(N)=14.532$ ev.[14] This gives EA(O) =1.47±0.05 ev. From his studies of CO, Lagergren[15] finds the appearance of zero kinetic energy C^+ and O^- ions at 20.95±0.05 ev, implying EA(O)=1.42±0.05 ev.

The previous[7,8] experimental determinations of the O^- photodetachment cross section suffered from rather low wavelength resolution. This limitation was imposed by the low signal-to-noise inherent in the experiment, which limited the accuracy of the threshold wavelength determination and prevented the use of monochromatic light to measure the wavelength dependence of the cross section.

The work reported here was initiated when improvements in the experimental techniques permitted independent measurements of the photodetachment cross section at different wavelengths and improved the accuracy of the measurement of the threshold wavelength by more than a factor of ten. The most important changes from the instrument described previously[8] are (a) the addition of a high-intensity mass analyzer which selects the ions before they enter the reaction chamber and (b) the introduction of a new optical system using a carbon arc source and band-pass interference filters to produce intense monochromatic radiation. The details of this apparatus will be described in a separate publication.

This paper describes (a) a precision determination of the oxygen electron affinity; (b) more reliable measurements of the photodetachment cross section at short wavelengths, to permit a more accurate extrapolation into the ultraviolet; (c) an investigation of the influence of the fine-structure splitting in the ground states of O^- and O; and (d) a more accurate calculation of the radiative attachment coefficient, which is very sensitive to the shape of the photodetachment curve near threshold.

THEORY OF O^- PHOTODETACHMENT

The ground state of O^- is ^2P arising from the configuration $(1s)^2(2s)^2(2p)^5$. In the photodetachment process one of the $2p$ electrons makes an electric dipole transition to a continuum orbital, which may be designated Ed or Es depending on which of the two allowed final angular-momentum states it occupies. The correct procedure for calculating the cross section for the process

$$h\nu+O^-(^2P)\rightarrow O(^3P)+e$$

requires the evaluation of the dipole matrix element between the bound and continuum states of a nine-electron atomic system. With the simplification that the total wave functions may be constructed from an appropriate combination of one-electron orbitals, the cross section is

$$\sigma(\lambda)=(16/3)\pi(k/\lambda)f_0(M_s^2+2M_d^2). \qquad (1)$$

All quantities are in atomic units; that is, σ is in units of πa_0^2, k is the electron wave number in units of $1/a_0$, and λ is the wavelength of the incident radiation in units of a_0. The factor f_0 represents the effect of the overlap integral of the core orbitals which remain bound in the transition. The radial dipole matrix elements are

$$M_s=\int_0^\infty P(2p|r)rP(Es|r)dr,$$

and

$$M_d=\int_0^\infty P(2p|r)rP(Ed|r)dr,$$

where P is r times the radial wave function.

This cross section has been calculated by several authors,[16–18] with results which differ rather widely from one another. The nature of these calculations will be discussed and compared with the experimental results near the conclusion of this paper.

For the analysis of the present data near threshold, it is convenient to know the theoretical shape of the cross-section curve in that region. To obtain this, we note that the asymptotic forms of the continuum functions are

$$P(Es|r)\rightarrow k^{-1}\sin(kr+\eta_0),$$

$$P(Ed|r)\rightarrow k^{-1}\left[\left(\frac{3}{k^2r^2}-1\right)\sin(kr+\eta_2)-\frac{3}{kr}\cos(kr+\eta_2)\right].$$

[7] Lewis M. Branscomb and S. J. Smith, Phys. Rev. **98**, 1127 (1955).
[8] S. J. Smith and L. M. Branscomb, J. Research Natl. Bur. Standards **55**, 165 (1955).
[9] H. D. Hagstrum, J. Chem. Phys. **23**, 1178 (1955).
[10] D. T. Vier and J. E. Mayer, J. Chem. Phys. **12**, 28 (1944).
[11] M. Metlay and G. E. Kimball, J. Chem. Phys. **16**, 744 (1948).
[12] E. M. Clarke, doctoral thesis, Universite Laval, Quebec, Canada (unpublished).
[13] L. Kerwin (private communication).
[14] *Atomic Energy Levels*, C. E. Moore, National Bureau of Standards Circular No. 467 (U. S. Government Printing Office, Washington, D. C., 1948), Vol. 1, p. 32. C. E. Moore (private communication) states that the value given in *Atomic Energy Levels*, Vol. 1, for $I(N)$ should be revised to $I(N)=14.532\pm0.001$ ev.
[15] C. R. Lagergren, doctoral thesis, University of Minnesota, 1955 (unpublished).
[16] D. R. Bates and H. S. W. Massey, Trans. Roy. Soc. (London) **A239**, 269 (1943).
[17] T. Yamanouchi, Proc. Phys.-Math. Soc. Japan **22**, 569 (1940).
[18] M. M. Klein and K. A. Brueckner, Phys. Rev. (to be published).

Since the atomic potential is short-ranged, we can consider an effective range r_0 at which the "inside" solutions are joined to the "outside" solutions given above. The s matrix element may be written as

$$M_s=\int_0^{r_0} P(2p|r)rP(Es|r)dr + k^{-1}\int_{r_0}^{\infty} P(2p|r)r\sin(kr+\eta_0)dr, \quad (2)$$

and similarly for M_d. In the limit of zero energy the lth phase shift, η_l, behaves[19] as

$$n_l\pi+k^{2l+1}(\beta_0+\beta_1k^2+\beta_2k^4+\cdots),$$

where n_l is an integer depending on the number of bound states of angular momentum $l\hbar$ that the potential can accommodate. If we consider a square well potential of depth D, the "inside" solution for the s-wave is

$$P(Es|r)=-\frac{1}{k}\frac{\sin(kr+\eta_0)}{\sin k'r_0}\sin k'r,$$

where $k'^2=k^2+(2m/\hbar^2)D$. If one substitutes this into (2), makes the series expansions for the trigonometric functions, and performs the integrations term-by-term, one finds

$$M_s \underset{k\to 0}{\longrightarrow} b_0+b_1k^2+b_2k^4+\cdots.$$

A similar treatment of the d-wave yields

$$M_d \underset{k\to 0}{\longrightarrow} c_1k^2+c_2k^4+\cdots.$$

The limiting form of the cross section near threshold becomes

$$\sigma \underset{k\to 0}{\longrightarrow} \frac{k}{\lambda}(a_0+a_1k^2+a_2k^4+\cdots). \quad (3)$$

Expressed in units of the detached electron energy E and the threshold photon energy E_0, this becomes

$$\sigma \longrightarrow (E_0+E)E^{\frac{1}{2}}(a_0'+a_1'E+a_2'E^2+\cdots). \quad (4)$$

The limiting forms of the dipole matrix elements have been obtained above with the aid of a square-well potential model, but they can be shown to hold for any short-range potential.

The photodetachment of electrons from atomic negative ions is one of the processes covered by Wigner's[20] general treatment of the threshold behavior of reactions having two final products. Since the interaction between the final products (e and O) is short-ranged, Wigner's result for "neutral particles" is applicable and gives $\sigma \longrightarrow k^{2l+1}$ as $k \longrightarrow 0$. The dipole selection rule for the transition of a bound p electron requires that $l=0$ or 2, giving the same limiting dependence on electron wave number as is obtained in (3). Only the coefficients in Eq. (4) depend on the bound-state wave functions and potential. The cross section is roughly parabolic in the ejected electron energy.

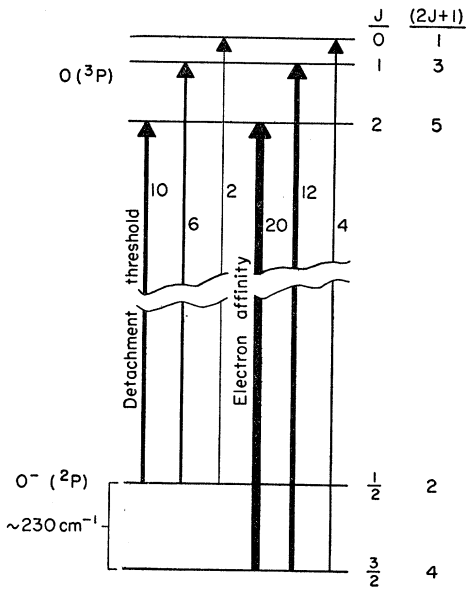

FIG. 1. Energy levels of O^- and the ground state of atomic oxygen. Each transition is labeled with the product of the statistical weights of the initial and final levels.

The expected shape of the photodetachment curve at the threshold is complicated by the fine-structure splitting of the ground states of both the negative ion ($^2P_{\frac{1}{2},\frac{3}{2}}$) and the neutral atom ($^3P_{0,1,2}$). These levels are sketched in Fig. 1. Thus we see that the actual detachment threshold, $O^-(^2P_{\frac{1}{2}}) \rightarrow O(^3P_2)$ occurs at a longer wavelength than the transition $O^-(^2P_{\frac{3}{2}}) \rightarrow O(^3P_2)$, which corresponds to the oxygen electron affinity.

To take this splitting into account in the interpretation of our photodetachment data, we must have an estimate of the magnitude of the O^- splitting. We find for this 230 cm^{-1}, or about 0.026 ev, from a polynomial extrapolation of the ground-state splittings of the isoelectronic atoms: F, Ne^+, Na^{++}, and Mg^{+++}. In the vicinity of 8500 A wavelength, this corresponds to about 160 A. For the relative population of the two ground-state components in our O^- beam, we assume a distribution proportional to the statistical weights of the states. The analysis of the experimental data then provides a numerical factor giving the ratio of the actual contribution of the splitting effect to that resulting from these rough estimates. From Fig. 2, we see that the expected effect of the splitting is small, and that it is closely approximated by adding to the detachment cross section *neglecting splitting* a small contribution 160 A wide and of magnitude 10/54 of the main curve.

[19] N. F. Mott and H. S. W. Massey, *The Theory of Atomic Collisions* (Clarendon Press, Oxford, 1949), second edition, p. 36.
[20] E. P. Wigner, Phys. Rev. **73**, 1002 (1948).

EXPERIMENTAL DETAILS

Photodetachment is detected experimentally by measuring the current of electrons which are detached when a beam of O^- ions is illuminated in high vacuum with intense visible or infrared radiation. The theory of the experiment, relating experimental quantities to the cross section, has been published previously.[21] Since only relative quantities were measured in the present work, it will suffice to use as the basic relation:

$$P_{\text{exp}}=\frac{i_{\text{elec}}}{I_{\text{ion}}}\propto v^{-1}\int\sigma(\lambda)\varphi(\lambda)T(\lambda)\lambda d\lambda. \tag{5}$$

Here P_{exp} is the experimental photodetachment probability per ion, defined as the ratio of electron current to ion beam current; v is the ion velocity; $\sigma(\lambda)$ is the photodetachment cross section; $\varphi(\lambda)d\lambda$ is the unfiltered radiant flux in a wavelength range λ to $\lambda+d\lambda$ at some point of the ion path through the radiation, and $T(\lambda)$ is the transmission function of an optical filter inserted in the light beam.

In previous studies of O^- photodetachment the signal-to-noise ratio did not permit the isolation of narrow bands of radiation, and it was necessary to determine $\sigma(\lambda)$ by solving a family of integral equations like (5). A number of optical filters were used which absorbed or reflected wavelengths shorter than selected cutoff wavelengths. With a certain filter $T^i(\lambda)$,

$$P_{\text{exp}}{}^i\propto v^{-1}\int\sigma(\lambda)\varphi(\lambda)T^i(\lambda)\lambda d\lambda. \tag{6}$$

The determination of $\sigma(\lambda)$ from data obtained with such a sequence of cutoff filters is tantamount to differentiating the data with respect to the cutoff wavelength and requires a very large signal-to-noise ratio. It also requires long-time stability of the spectral distribution of the source, precluding the use of high-intensity carbon arcs.

In the present experiment two methods, using different applications of Eq. (5), were used to determine $\sigma(\lambda)$. The first of these methods is applicable only when the cross section is a slowly varying function of wavelength, while the second can be used only in the vicinity of threshold. The regions of validity of the methods do not quite overlap in the case of O^-, but a sensible joining of the results can be effected.

Method I

For photon energies more than 0.2 ev above the photodetachment threshold the cross section changes sufficiently slowly that selected bands of radiation, about 500 A wide, were used to find $\sigma(\lambda)$ directly. When monochromatic radiation can be used, one has

$$W(\lambda)=\varphi(\lambda)T(\lambda)\propto\delta(\lambda-\lambda'),$$

[21] L. M. Branscomb and S. J. Smith, Phys. Rev. **98**, 1028 (1955).

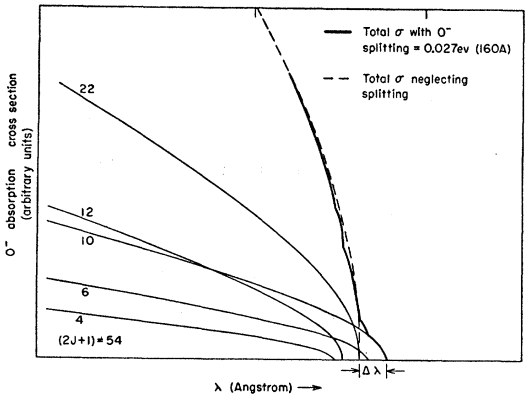

FIG. 2. Contributions to the total photodetachment cross section *vs* photon energy from the transitions depicted in Fig. 1. The total cross section, neglecting the toe, is closely approximated by the dotted curve, which has the same analytic form as that of the separate contributions.

where λ' is the wavelength of the monochromatic light. Then Eq. (5) can be altered and rearranged to read

$$\sigma(\lambda')\propto P_{\text{exp}}v/\lambda' W_t, \tag{7}$$

in which W_t is the measured radiant power proportional to the integral of $W(\lambda)$ over wavelength. If the experimental spectral radiant power function, $W(\lambda)$, is not precisely monochromatic but $\sigma(\lambda)$ varies linearly over the range of wavelength of the filter involved, the value of the cross section at the second moment, λ_2, of $W(\lambda)$ is

$$\sigma(\lambda_2)\propto P_{\text{exp}}v/\lambda_1 W_t, \tag{8}$$

where λ_1 is the first moment, or center of gravity, of $W(\lambda)$.

In this spectral range W was monitored by a bolometer. A sheet of clear Corex D glass, placed at an angle in the converging beam of filtered radiation, reflected about 8% of the light into a small white integrating sphere. The bolometer measured the intensity of integrated light in this sphere. The entire optical system was carefully calibrated to minimize wavelength-dependent systematic errors in the radiometry.

Typical filter transmissions are shown in Fig. 3. The wavelength range covered by these filters is 0.4 to 2.4 μ. With a 30-ampere carbon arc producing a 1-cm$\times$2-cm image in an $f/1.5$ optical system, a filter combination transmitting in the visible region of the spectrum would illuminate the ion beam with about one watt of chopped radiation. About 10^{-8} amp of 300-ev O^- ions would then produce a photodetachment current of the order of 10^{-14} amp. The signal-to-noise ratio under these conditions is limited by the noise in the electron current produced by collisional detachment by the residual gas atoms in the reaction chamber, and would be about 20 with a typical vacuum of 2×10^{-7} mm Hg.

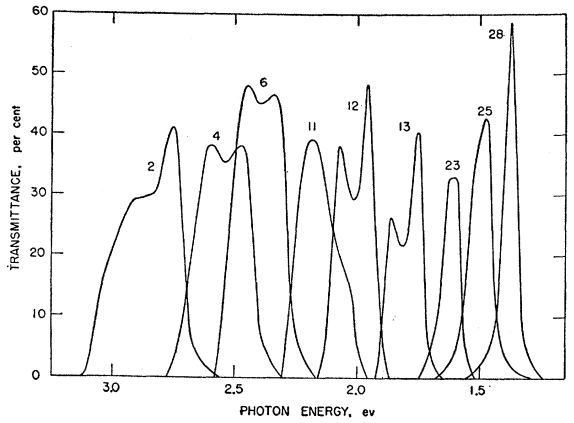

FIG. 3. Curves of transmittance *vs* photon energy of typical band-pass filter combinations of the type used in Method I discussed in the text.

Method II

Very near the threshold (within about 0.2 ev) the cross section changes too nonlinearly over the width of one of the band-pass filters for (7) to represent a close approximation to $\sigma(\lambda)$. On the other hand, the spectral distribution of the carbon arc is very nearly constant over the narrow wavelength range from 0.75 μ to threshold. This permits Eq. (6) to be written

$$P_{\exp}{}^{i} \propto \Phi v^{-1} \int \sigma(\lambda) T^{i}(\lambda) \lambda d\lambda, \tag{9}$$

where Φ is the mean value of $\phi(\lambda)$ in the 0.1-μ interval. The arc intensity is then monitored before the radiation is filtered. The filters whose transmittances are shown in Fig. 4 are then interposed in the light beam, and the negative-ion detachment probability $P_{\exp}{}^{i}$ is then measured for each of the seven filters. The transmittances $T^{i}(\lambda)$ were very carefully measured on a Cary spectrophotometer, with special attention being given to the effect of internal reflections between the filters.

To find the threshold shape of $\sigma(\lambda)$ we must solve seven simultaneous integral equations like (9). These do not give a unique solution for the cross section, if we admit sufficiently complex functions for $\sigma(\lambda)$. Hence, we must take certain assumptions if we are to obtain a unique experimental determination of the threshold shape and wavelength. We assume (a) that the theoretical threshold expansion, Eq. (4), converges sufficiently rapidly so that it is adequately represented over the first 0.1 ev above threshold with a_2' and all higher coefficients set equal to zero, and (b) that the extrapolated value for the ground-state splitting of O^- is adequate. These assumptions lead to the following form of the photodetachment cross section near threshold:

$$\sigma(\lambda) = \frac{10}{54}\left(\frac{\gamma B}{\lambda}\right)\left[\frac{(\lambda_1-\lambda)}{\lambda_1\lambda}\right]^{\frac{1}{2}} \quad \text{for} \quad \lambda_0<\lambda<\lambda_1$$

$$= \left(\frac{\gamma}{\lambda}\right)\left[\frac{(\lambda_0-\lambda)}{\lambda_0\lambda}\right]^{\frac{1}{2}}$$

$$+\left(\frac{\gamma A_1}{\lambda}\right)\left[\frac{(\lambda_0-\lambda)}{\lambda_0\lambda}\right]^{\frac{3}{2}} \quad \text{for} \quad \lambda<\lambda_0, \tag{10}$$

in which γ is a constant of proportionality, B is a factor introduced to compensate for the uncertainty in the relative populations of the $^2P_{\frac{1}{2}}$ and $^2P_{\frac{3}{2}}$ states of O^-, and λ_0 and λ_1 are respectively the wavelengths of onset of photodetachment from the $^2P_{\frac{3}{2}}$ and $^2P_{\frac{1}{2}}$ states. If more terms of Eq. (4) were used in the construction of (10), constants A_2, A_3, etc., would appear corresponding to a_2', a_3', etc.

As we shall see in subsequent discussion, it is not experimentally feasible to determine higher order coefficients A_2, A_3, etc., from the available data. However, we are encouraged by two circumstances to use the relatively simple form of Eq. (10). First, all of the theoretical calculations of the O^- photodetachment cross section have given results which are accurately fit by (10) over the first tenth of an electron volt using a small value of A_1 and no higher coefficients. Secondly, if the actual cross section cannot be approximated by this threshold form, the statistical analysis of the data would reveal this fact. But, as will be seen, values of the parameters can be found for which (10) is in excellent agreement with the data. Should some theoretical evidence be developed that the curve should have a more complex structure at threshold, the experimental data can be used to test the acceptability of the proposed shape.

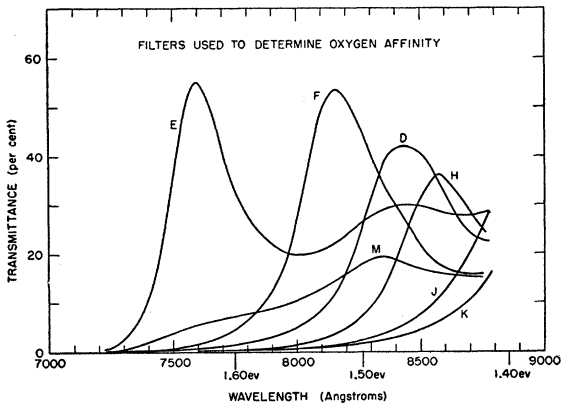

FIG. 4. Curves of transmittance *vs* photon wavelength of filter combinations used in Method II discussed in the text.

RESULTS AND DISCUSSION

Results from Method I

The values of the O^- photodetachment cross section obtained with the band-pass filters are shown as points in Fig. 5. Each point is the average value obtained from a number of measurements with a band-pass filter, and the associated error bar shows the root-mean-square deviation of the measurements from the average value for that band-pass filter. The results do not demonstrate the existence of structure. The dashed line is the most reasonable curve for the cross section.

The experiment as performed gives relative values of cross section. These were put on an absolute scale for presentation in Fig. 5 by comparison of the data with the absolute integrated cross sections previously measured.[8] In the earlier experiment the detachment probabilities from O^- were measured by using radiation from a 1-kw wolfram projection lamp filtered with a series of Corning sharp-cutoff absorption filters. There the proportionality in Eq. (5) was made an equality by absolute measurement of the spectral radiant flux, the ion velocity, and the geometrical constants. We now introduce the presently obtained relative cross section into the integrals [Eq. (5)] corresponding to the several filters used in the earlier experiment. The normalization factor which makes these integrals equal to the previously measured detachment probabilities then serves to put the present measurements on an absolute basis.

To provide a check on the normalization, we made an experimental measurement of the ratio of photodetachment probabilities of O^- and D^- with a narrow band-pass filter centered at 5375 A. This ratio is 0.20 ± 0.03, giving $\sigma(D^-)=(3.18\pm0.48)\times10^{-17}$ cm^2. This result is consistent with both the theory of Chandrasekhar[22] ($\sigma=3.59\times10^{-17}$ cm^2) and that of Geltman[23] ($\sigma=3.38\times10^{-17}$ cm^2) at this wavelength. This agreement between an experimentally measured value of $\sigma(D^-)$ and a value given by a theory for which the integrated cross section has been shown previously to be correct[21] indicates the correctness of the procedure used in normalizing the relative $\sigma(O^-)$ data to an absolute scale.

TABLE I. Experimental photodetachment probabilities.

Filter	P^{exp}_i ($P^i\pm\Delta P^i$)
E	1.665±0.023
F	1.000±0.015
M	0.503±0.009
D	0.415±0.007
H	0.142±0.004
J	0.053±0.003
K	0.037±0.002

[22] S. Chandrasekhar, Astrophys. J. **102**, 395 (1945).
[23] S. Geltman, Phys. Rev. **104**, 346 (1956).

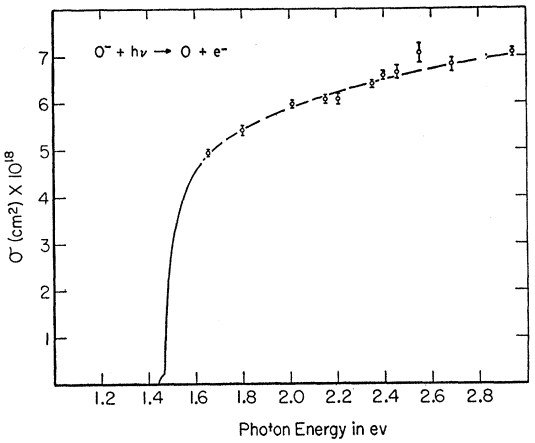

FIG. 5. Photodetachment cross section of atomic-oxygen negative ions *vs* photon energy. The dotted line is drawn to pass through the points which were obtained by Method I described in the text. The solid line was deduced by making use of Method II. The small projection at the threshold region is due to the assumed splitting in the ground state of O^-.

Results from Method II

The electron affinity and the cross section between threshold and 1.575 ev were determined from the second method described in the section on experimental details. Table I shows the experimental probabilities resulting from use of the filters whose transmittances are depicted in Fig. 4. Since these data were analyzed by statistical methods, some description of the procedure for assigning errors is pertinent. The data of Table I were collected in two runs on separate days, between which the equipment had been totally shut down. In both runs the filters were used in a cyclic order designed to reveal any systematic variation of experimental conditions. In the first run each filter was used five times. The results for each filter were averaged and the unweighted standard errors of the mean were calculated. In the second run, each filter was used to make a group of from one to seven measurements taken in immediate succession. Five such groups were obtained for each filter. The group averages and mean deviations were computed. The average over groups was then calculated for each filter and the standard errors were obtained from the group mean deviations weighted by the number of measurements constituting the group. Finally, the results of the two runs were averaged and the square root of the sum of the squares of the standard errors for the two runs was attached as the error, ΔP^i.

The factors which multiply γ, γA_1, and γB in Eq. (10) were calculated for five values of λ_0 in the neighborhood of 0.845 μ (1.467 ev) and for a range of λ from λ_0 to 0.700 μ. Each case of Eq. (10) so calculated was then multiplied by λ and the seven filter transmittance curves. Each resulting function was integrated, as indicated by Eq. (9), by the use of Simpson's rule

with intervals of 0.005 μ. A set of seven "theoretical" probabilities for photodetachment,

$$p^i=\gamma F_0{}^i+\gamma A_1 F_1{}^i+\gamma B F_s{}^i, \tag{11}$$

was thus obtained for each λ_0. Here the three F's result from the λ integrations over the three terms of Eq. (10). The problem was now continued by machine methods. A least-squares adjustment of the p^i to the experimental probabilities P^i was performed for each value of λ_0. The results of the adjustment were the values of γ, γA_1, and γB giving the best fit at each λ_0, and the standard error $S(\lambda_0)$ of the fit. The quantity $S(\lambda_0)$ is defined by

$$S=\left(\frac{1}{n-m}\sum_{i=1}^{n}\delta_i{}^2 w_i\right)^{\frac{1}{2}},$$

where the δ_i are the deviations of the p^i from the P^i, w_i are the weights used in the calculation $[w_i=10^{-6}/(\Delta P^i)^2]$, n is the number of data, and m is the number of constants to be determined. Since the weights are proportional to the squares of the reciprocals of the experimental errors, the experimental quantity to be compared with the $S(\lambda_0)$ values is

$$S_{\text{exp}}=\left[\frac{1}{n-m}\sum_{1}^{n}(10^{-6})\right]^{\frac{1}{2}}=\left(\frac{n}{n-m}\right)^{\frac{1}{2}}\times 10^{-3}.$$

Figure 6 is a plot of $S(\lambda_0)$ for several programs of computation. Figure 6(a) indicates the result when $A_1=0$ is entered as input information. In this case $n=7$ and $m=2$, whence $S_{\text{exp}}=1.18\times 10^{-3}$. $S(\lambda_0)$ has a minimum in the region of 0.847 μ but is everywhere larger than S_{exp}. Therefore a nonvanishing value for A_1 must be used. To obtain Fig. 6(b), A_1 also was allowed to vary.

Now $m=3$ and $S_{\text{exp}}=1.32\times 10^{-3}$. We see that the fit is greatly improved and that all values of λ_0 between 0.845 and 0.850 μ can be consistent with experiment. From this fit the best values of A_1 and B are determined to be -2.7 μ and 0.06 (dimensionless), respectively, at $\lambda_0=0.8475$ μ. This value of A_1, however, gives a maximum for Eq. (9) at $\lambda\sim 0.75$ μ while the point-by-point data indicate a decreasing cross section.

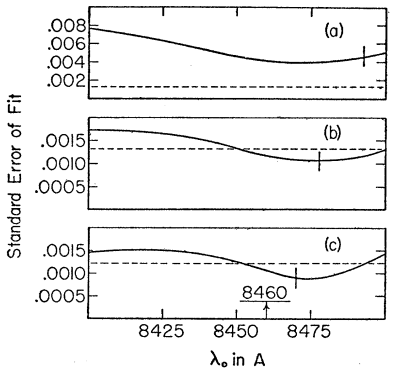

FIG. 6. Variation with onset wavelength λ_0 of standard error of fit of Eq. (10) to data of Table I for three programs of computation: (a) $A_1=0$; (b) A_1 determined by fit; (c) same as (b) but with data of filter E deleted. In each case the dashed line represents the experimental error. The part of the curve to the right of the vertical bars corresponds to the physically excluded condition $B<0$.

It may be seen from Fig. 4 that a considerable part of the area under the transmission curve for filter E lies above an energy greater than 0.1 ev above threshold. To check the effect on the data of filter E, the calculation was reprogrammed with weight zero given P^E. The result is depicted in Fig. 6(c) and it is clear that P^E is relatively unimportant in determining λ_0, since all values of the latter between 0.845 and 0.849 μ are capable of satisfying the experimental data. However, the fit for λ_0 greater than 0.847 μ is best for negative values of B, which are physically inadmissible. Accordingly, we take the best value of λ_0 to be the midpoint of the remaining acceptable interval, $\lambda_0=0.846$ μ.

The restrictions imposed by requiring $B\geqslant 0$ and $S(\lambda_0)\leqslant S_{\text{exp}}$ give limits of error on λ_0 of ~ 0.001 μ. However, it must be remembered that Eq. (10) is an approximation and the inclusion of more terms may give larger limits between which λ_0 may vary. We do not expect the width of the acceptable range of the $S(\lambda_0)$ curve to increase appreciably, provided experimental errors in determining the coefficients of terms added to (10) are not important (see below). Nevertheless, we prefer to extend the limits of error of λ_0 to three times the value given above, feeling that this should allow for all contingencies. Accordingly, our result for the threshold wavelength is

$$\lambda_0=0.846\pm 0.003\ \mu,$$
$$\text{EA(O)}=E_0=1.465\pm 0.005\ \text{ev}.$$

An attempt to refine the calculation further by appending a term $(\gamma A_2/\lambda)[(\lambda_0-\lambda)/\lambda_0\lambda]^{\frac{5}{2}}$ to the part of Eq. (10) valid when $\lambda\leqslant\lambda_0$ was made, but the results did not constitute an improvement. In order that the extra term be sufficiently accurate to warrant its use in determining λ_0, the transmissions of some of the filters must be known accurately in regions where they are as small as 0.01%. Also, the requirement that another parameter be determined raises S_{exp} more than $S(\lambda_0)$; all values of λ_0 between 0.840 and 0.850 μ can be consistent with the experiment provided sufficiently extreme values of A_1, A_2, and B are used. At $\lambda_0=0.846$ μ the best fit occurs with $A_1=-4.2\mu$, $A_2=10.7\mu^2$, and $B=0.3$. Equation (10) with the extra term added and with these values for the parameters is plotted in Fig. 5 (solid line) where it has been normalized to fit smoothly into the point-by-point data.

In summary, we find an electron affinity of 1.465 ± 0.005 ev, and a photodetachment curve of the general form given in Fig. 5. In the threshold region we find the data consistent with the expansion of Eq. (4), with a_1' negative and the signs of subsequent terms

alternating. The effect of the fine structure is small, and we have only shown that B is less than one. It has been necessary to include the effect in the analysis; otherwise the accuracy of the affinity determination would have been overestimated.

Comparison of Experiment with Theory

The O^- photodetachment cross section has been evaluated by several authors[16–18] over the region of wavelengths covered by the present experiment. The results of the two older calculations were presented on the basis of an electron affinity of oxygen of 2.2 ev.[1] It is very simple to correct their results to the present affinity of 1.465 ev, since the matrix elements depend only on the total electron energy (or photon energy above threshold) and not on the photon wavelength. These affinity-corrected theoretical curves and the experimental curve are plotted in Fig. 7. The large divergence of the three calculated curves, both with respect to shape and magnitude, indicates how sensitive their results are to the approximate wave functions used. Thus, it is worth briefly reviewing the underlying approximations in each of the calculations.

Both Yamanouchi[17] and Bates and Massey[16] use the O^- Hartree-Fock function for $P(2p|r)$; hence the effect of exchange between the bound electrons is included. Bates and Massey's $P(Es|r)$ is a solution of the radial wave equation with exchange using the Hartree-Fock field of O in the ^3P state plus a polarization-type potential based upon a calculated polarizability of O. Yamanouchi obtains $P(Es|r)$ using a Hartree-Fock field which has been averaged over the ^3P, ^1D, and ^1S states which arise from the ground configuration of O. The difference between the ^3P and the mean Hartree-Fock field is insignificant. These two calculations use $f_0 \cong 0.9$, and $P(Ed|r)$ is obtained from the d radial wave equation without exchange.

The approach of Brueckner and Klein[18] is to employ an oxygen atom potential consisting of the Hartree-Fock field plus a polarization field with a polarizability parameter adjusted so as to yield a bound p level, of binding energy 1.45 ev.[7] The polarizability determined in this way agrees surpisingly well with the previously calculated[16] value of this parameter for the oxygen atom. The ground and $P(Es|r)$ continuum radial functions are both calculated from this potential and all effects arising from the core electrons are ignored, i.e., $f_0=1$. $P(Ed|r)$ was approximated by the corresponding field-free radial function. This approach has the advantage that the length, velocity, and acceleration forms of the dipole matrix element are equal.[22,23] Exchange is not explicitly considered in the Brueckner and Klein calculation, but it may be implicitly accounted for (in bound states) by the requirement that the potential yield an eigenvalue at the observed binding energy.

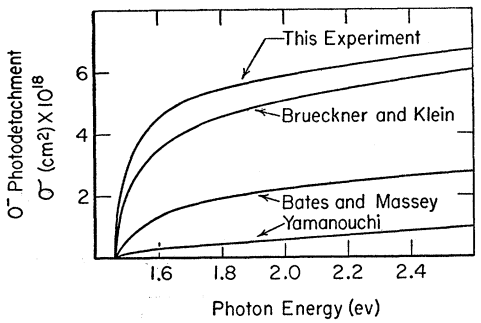

FIG. 7. Comparison of experiment with various theories for the photodetachment cross section of O^-.

Radiative Attachment to Oxygen Atoms

The principle of detailed balancing[24] provides a means of determining the radiative attachment cross section from the photodetachment cross section. The radiative attachment coefficient, defined as the product of electron velocity and attachment cross section, is given as

$$\alpha = 58.07 E^{-\frac{1}{2}}(E+E_0)^2(g_-/g_0)\sigma_{\text{det}}(E), \qquad (12)$$

where E is the electron energy, E_0 is the energy with which the electron is bound in the ion, g_- and g_0 are the statistical weights of the ground states of ion and atom respectively, and $\sigma_{\text{det}}(E)$ is the photodetachment cross section expressed as a function of energy of the detached electron. The quantities E and E_0 are in electron volts and $\sigma_{\text{det}}(E)$ in cm^2.

As discussed earlier, the ground state of O^- is split into two components with J values of $\frac{1}{2}$ and $\frac{3}{2}$, while there are three components of the ground state of the neutral atom, 0, 1, and 2. The statistical weights are 2 and 4 for the states of O^- and 1, 3, and 5 for the states of O. Now earlier it was assumed that, except for the small toe appended to the main part of the curve, the total photodetachment cross section combining all transitions between the different levels could be closely approximated by a single smooth curve with the same analytic form. The assumption is equivalent to neglect of the splitting for the region of the curve at photon energies above E_0. The values of g are then the sums for atom and ion; $g_0=9$ and $g_-=6$. Neglect of the attachment from the lowest state of O into the upper state of O^- for electrons of energy less than the splitting of the levels will cause an error of the same order as that introduced by the assumption discussed above. The effect of the toe was therefore deleted in the calculation of α.

The result of a calculation of (12), using $\frac{2}{3}$ for g_-/g_0 and the composite curve of Fig. 5 for the photodetachment cross section (neglecting the toe), is given in Fig. 8. Note that the abscissa of Fig. 5 is photon

[24] J. D. Jackson, National Research Council Report No. 2610, Chalk River, Ontario, 1951 (unpublished), p. 2ff.

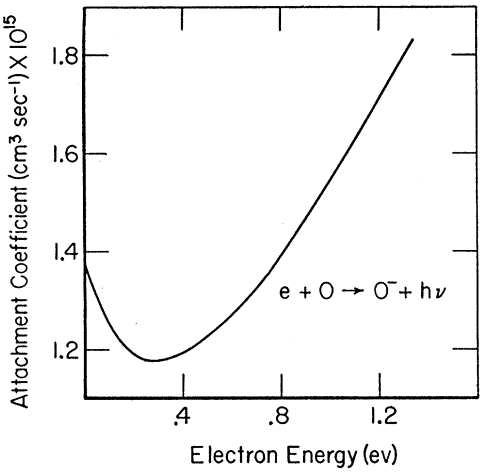

FIG. 8. Coefficient of attachment of electrons to oxygen atoms *vs* electrons energy.

energy and must be converted to electron energy (by reduction by 1.465 ev) for use in Eq. (12).[25]

If the limiting form for σ_{det} from Eq. (4) with a proportionality constant β be used in Eq. (12), the attachment coefficient may be written

$$\alpha=38.71\beta(E+E_0)^3[1+0.807A_1E + (0.807)^2A_2E^2\cdots]. \quad (13)$$

With our normalization and values for A_1, A_2, and E_0, the constant of proportionality of Eq. (4) is $\beta=1.08\times10^{-17}$ cm^2. At $E=0$,

$$\alpha=38.71\beta E_0^3=1.31\times10^{-15}\text{ cm}^3\text{ sec}^{-1}.$$

If Eq. (13) be differentiated, the initial slope is found to be

$$(d\alpha/dE)_{E=0}=38.71\beta E_0^2(3+0.807A_1E_0) \quad (14)$$

and, for our values of β and E_0

$$(d\alpha/dE)_{E=0}=0.879(3+1.182A_1)\times10^{-15}\text{ cm}^3\text{ sec}^{-1}\text{ ev}^{-1}. \quad (15)$$

It will be observed that the initial slope is quite sensitive to the value of A_1, the logarithmic slope $(1/\alpha)(d\alpha/dE)|_{E=0}$ having the value zero for $A_1=-2.54$ μ, and -1.34 ev^{-1} for our value of $A_1=-4.2$ μ.

For purposes of calculation of upper atmosphere formation of O$^-$,[26,2,3] we have calculated the temperature dependence of the mean radiative attachment coefficient for oxygen atoms in a gas of electrons with a Maxwellian distribution. The result of this calculation is displayed in Fig. 9.

CONCLUDING REMARKS

There are numerous applications of the results of this experiment to associated problems of physics. We shall mention briefly only four: the determination of EA(C), calibration of appearance-potential scales in mass spectroscopy, the midday concentration of O$^-$ in the upper atmosphere, and the rate of production of O*(^1S) and O*(^1D) by photodetachment in the upper atmosphere.

Lagergren[15] has determined experimentally a relation between the electron affinities of carbon and oxygen:

$$\text{EA(O)}-\text{EA(C)}=0.35\pm0.05\text{ ev}.$$

Making use of the value of EA(O) given above, we find

$$\text{EA(C)}=1.12\pm0.05\text{ ev}.$$

The appearance potential for an ion produced by a certain reaction is defined as the minimum electron energy required to produce the ion in an electron-molecule collision. Mass spectroscopic studies of negative ions have been hampered by a paucity of the spectroscopic data needed to establish a calibration of the equipment used in such studies. One of us[27] has prepared a note which explains in detail how the value of EA(O) reported above may be combined with other spectroscopic data to provide a calibration of negative-ion appearance potential scales using thresholds for ion pair formation in CO, NO, or O_2.

The mean attachment coefficient $\bar{\alpha}$ shown in Fig. 9 can be utilized along with models of the upper atmosphere[28,29] and data on electron densities obtained by vertical radio soundings[30] to obtain the rate of production of O$^-$. The results indicate that the rate is greatest at heights of ~100 km above middle latitude at noon on a summer day when its value is ~90 cm^{-3} sec^{-1}. The photodetachment cross section shown in Fig. 5 can be

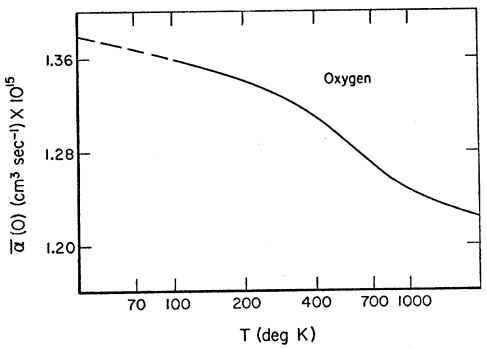

FIG. 9. Mean attachment coefficient *vs* temperature in atomic oxygen for a Maxwellian distribution of electron energies.

[25] We wish to call attention to an error in the presentation of a curve of α published previously. In Fig. 10 of the article in reference 8, and in Fig. 8 of the article in reference 2, curve *A* should be moved to the left by 1.48 ev and the portion of the curve which then lies in the negative-energy region should be deleted.

[26] L. M. Branscomb and S. J. Smith, Trans. Am. Geophys. Union **36**, 755 (1955).

[27] L. M. Branscomb (to be published).

[28] Kallman, White, and Newell, J. Geophys. Research **61**, 513 (1956).

[29] M. Nicolet and P. Mange (private communication).

[30] *Ionospheric Radio Propagation*, National Bureau of Standards Circular No. 462 (U. S. Government Printing Office, Washington 25, D. C., 1948), p. 38 ff.

combined with data on the solar flux[31] to calculate the rate at which this process destroys O^- in the atmosphere. The rate is found to be $\rho \sim 1.4$ per negative ion per second at noon. If photodetachment is the dominant process of those responsible for destruction of O^- in the upper atmosphere, then, under steady state conditions, the density of O^- is

$$n(O^-) \sim 64 \text{ cm}^{-3},$$

at the location and time described above.

Radiation from the upper atmosphere resulting from the processes

$$O^*(^1S) \rightarrow O^*(^1D) + h\nu,$$
$$O^*(^1D) \rightarrow O(^3P) + h\nu,$$

has often been observed.[32] Photodetachment of the atomic oxygen ion may help provide the population of excited states in twilight periods. Multiplying the right side of Eq. (1) by the ratio of statistical weights of $O(^3P)$ and $O^*(^1S)$ or $O^*(^1D)$ alters the equation to make it appropriate to the processes resulting in the excited states of the atom. The product $f_0(M_s^2+2M_d^2)$ for $O^- \rightarrow O(^3P)$ can be calculated from the data displayed in Fig. 5. A knowledge of the energy differences between the excited and ground states of the atom from spectroscopic data then allows computation of the cross sections for the processes giving the atoms in their excited states, provided we assume that $f_0(M_s^2+2M_d^2)$ does not change appreciably from its ground-state value. These cross sections are plotted in Fig. 10. In combination with the data on solar flux[33] we find, again at noon,

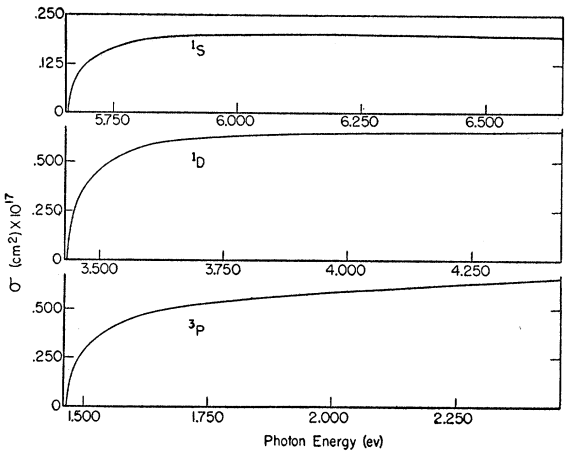

FIG. 10. Photodetachment cross sections *vs* photon energy for processes leading to different final states of the oxygen atom.

$$\rho(^1S) = 0.78 \times 10^{-4} (\text{negative ion})^{-1} \text{ sec}^{-1},$$
$$\rho(^1D) = 0.77 \times 10^{-1} (\text{negative ion})^{-1} \text{ sec}^{-1}.$$

ACKNOWLEDGMENTS

The authors wish to express their gratitude to numerous colleagues and friends who have been particularly generous of their time and talents. We would like to give special thanks to John Gould, Harry Keegan, John Schleter, Milton Abramowitz, Joseph Cameron, Mary C. Dannemiller, Adolphe P. Huriaux, and Robert Pearlstein, all of whom gave invaluable assistance in the preparation for the experiment or analysis of its results.

[31] *Smithsonian Physical Tables* (Smithsonian Institution, Washington, D. C., 1954), p. 722.

[32] S. K. Mitra, *The Upper Atmosphere* (Royal Asiatic Society of Bengal, Calcutta, 1947), first edition, p. 470.

[33] R. Tousey, *The Solar System* (University of Chicago Press, Chicago, 1953), first edition, Vol. 1 (*The Sun*), p. 665.